Chalcogenide Letters Vol. 16, No. 12, December 2019, p. 577 - 586

EFFECT OF DEPOSITION PARAMETERS ON THE COMPOSITIONAL AND OPTICAL PROPERTIES OF Cu_2SnS_3 THIN FILMS PREPARED BY CHEMICAL BATH DEPOSITION

M. F. A. ALIAS[a,*], B. Y. TAHER[b], I. S. NAJI[a], S. IQBAL[c], A. KAYANI[c],
M. F. MABROOK[d], A. A. J. AL-DOURI[e]
[a]*Department of Physics, College of Science, University of Baghdad, P.O. Box 47162,Jadiriyah,Baghdad, Iraq*
[b]*College of Agriculture, University of Anbar, Iraq*
[c]*Physics Department, Western Michigan University, Kalamazoo, USA*
[d]*School of Electronic, Engineering, Bangor University, UK*
[e]*Department of Applied Physics and Astronomy, College of Sciences, University of Sharjah, Sharjah, UAE*

We investigated properties of Cu_2SnS_3 thin films prepared on glass substrates by chemical bath deposition. The effect on elemental composition and optical properties of deposition parameters, such as substrate temperature (T_s= 313 K, 323 K, 333 K and 343 K) and pH value of the chemical bath (1.0, 1.5 and 2.0), while using fixed deposition time of 80 minutes are reported. The composition, thickness and optical properties of the thin films were investigated using Rutherford backscattering spectrometry and UV-vis spectroscopy, respectively. The thicknesses of the prepared films fluctuated with the pH; however the temperature has not clear effect on the thickness. The compositional analysis showed that most of the samples were Cu rich and S poor with respect to stoichiometric Cu_2SnS_3. The films prepared at T_s = 343 K exhibited real phase composition in the range of 56-72%, depending on the solution pH. The optical energy direct transition band gap of the films ranged from 2.48 to 2.58 eV, depending on the deposition parameters. Thin film deposited at 343 K and pH = 2 showed the best optical properties, which makes it a suitable candidate for the fabrication of photovoltaic devices.

(Received March 22, 2019; Accepted December 1, 2019)

Keywords: Copper-tin-sulphide, Thin films, Chemical bath deposition,
Rutherford backscattering spectrometry, Optical band gap, Refractive index,
Extinction coefficient

1. Introduction

In recent years, the ternary semiconductor, copper tin sulphide Cu_2SnS_3 (CTS), has received a great deal of attention. This is because it is composed of abundant and low cost elements that are recognized as being environmentally safe [1,2]. Thin CTS films are applicable in different technological fields, such as solar cells (as a good absorber material because of their high absorption coefficient $>10^4$ cm^{-1}); photoconductors devices; UV light emitting diode; and electroluminescent [3,4].

Cu_2SnS_3 belongs to the I_2-IV-VI_3 layered semiconductor family, having variety of interesting characteristics , such as low melting point, and high refractive index [5]. There are many techniques have been used to prepare thin CTS films with different phases, such as sulfurizing stacked metal precursors [6], radio-frequency (RF) magnetron sputtering [1], the solvothermal method [7], spray pyrolysis [8], hydrazine solution processing [2], thermal co-evaporation [9,10], electrodeposition [11], cyclic voltammetry [12], and the chemical bath deposition technique (CBD) [13 -15]. Among these, the CBD technique has several advantages [11,16], such as since it is 1) relatively inexpensive, 2) can be applied to large areas, 3) requires

---

[*] Corresponding author: may20131313@yahoo.com

low temperature processing, and 4) does not require sophisticated instrumentation. Moreover 5) the thickness of the film can be controlled and 6) the films adhere well to the substrate.

In this paper, we report the effects of the deposition temperature, pH values and fixed deposition time on the elemental composition, thickness and optical properties of deposited thin films. The deposition parameters have modulated to identify the best fabrication parameters among the ones tested.

2. Experimental

Nano thin CTS films were deposited on a 76mm × 26mm × 1 mm clean glass slide using a CBD technique. The solutions were prepared using deionised water and the chemical compounds used were copper sulfate ($CuSO_4.5H_2O$), tin chloride ($SnCl_2.2H_2O$), sodium thiosulfate ($Na_2S_2O_3.5H_2O$), and disodiumethylenediaminetetraacetic ($Na_2EDTA.2H_2O$). Copper sulfate, tin chloride, and sodium thiosulfate were used as a source of copper, tin, and sulfate ions, respectively. Na_2EDTA was used as a complex agent with Cu^{2+} and Sn^{2+} to obtain Cu-EDTA and Sn-EDTA complex solutions. The presence of the complex agent EDTA in the solution helped to improve the adhesion of the deposited films on the glass substrates. The ratio used for Cu, Sn and S to obtain CTS films was 2:1:3, respectively. Details of the fabrication process can found in our previous work [17]. Thin CTS films were fabricated with different fabrication parameters (T_s=313, 323, 333 and 343 K), and different acidity parameters (pH=1, 1.5 and 2) at a constant deposition time of 80 minutes. This mean there were 3 samples for each substrate temperature. In order to identify them, the samples were named to indicate the substrate temperature and pH value used for the deposition process, where symbols (L, M, N, and R) represent substrate temperatures (T_s=313, 323, 333, and 343 K), and (A, B, and C) represent pH values (1, 1.5, and 2), respectively. For example, the sample Ts313,pH1.0 was deposited at 313 K and pH 1.0, also by symbol LA.

The elemental composition and relative thickness of the samples were obtained via Rutherford Backscattering Spectrometry (RBS) measurements taken at Western Michigan University's particle accelerator lab using a 6 mega Volt Van De Graaff accelerator. For RBS, a He^{++} ion beam of energy 2.5 MeV was used and backscattered ions were detected using a surface barrier silicon detector at the 150^o scattering and 30^o exit angles. The RBS data was simulated using SIMNRA [18], and elemental composition and thickness were obtained from this simulation. UV/Vis optical measurements at room temperature of deposited films were obtained using a UV-Vis spectrophotometer model 6800 JENWAY with scan range of wavelength between 350-750 nm. From the absorbance measurements, optical parameters, such as optical energy gap (E_g), absorption coefficient (α), refractive index (n), extinction coefficient (κ), real (ε_r) and imaginary (ε_i) dielectric constants, optical conductivity (σ_{op}), were then calculated using the equations explained below:

Taking the absorption spectra, the absorption coefficient has been obtained directly by using Beer-Lambert law:

$$\alpha = 2.303\left(\frac{A}{t}\right) \tag{1}$$

where A is the absorbance and t is the thickness of the film.

The theory of reflectivity of light was used to calculate the value of the refractive index (n) and extinction coefficient (κ) [19].

$$\kappa = \frac{\alpha\lambda}{4\pi} \tag{2}$$

$$n = \frac{R^{1/2}+1}{1-R^{1/2}} \tag{3}$$

where λ is the wavelength and R is reflectance. The fundamental absorption edge follows an exponential law above the exponential tail; the absorption coefficient was assumed to obey the following equation [20]:

$$\alpha h\upsilon = B(h\upsilon - E_g)^r \tag{4}$$

where B is inversely proportional to amorphousity [21,22], hυ is photon energy and r is an exponent, which can be assumed to have values of 1/2,3/2, 2 and 3, depending on the nature of the electronic transition responsible for the absorption. $r = 1/2$ for allowed direct transition, $r = 3/2$ for forbidden direct transition, $r = 2$ for indirect allowed transition and $r = 3$ for forbidden indirect transition. The direct energy gap was calculated by plotting $(\alpha h\upsilon)^2$ as a function to photon energy of the film. The optical energy gap values are obtained by extrapolating the linear portion of the plots to intercept the photon energy axis.

The complex dielectric constant is a fundamental material property. The real part of it is understood in terms of how much it will slow down the speed of light in the material. The imaginary part gives information about how a dielectric absorbs energy from the electric field due to dipole motion. The real (ε_r) and imaginary (ε_i) parts of the dielectric constants were determined using the relations [23]:

$$\varepsilon_r = n^2 - k^2 \tag{5}$$

$$\varepsilon_i = 2nk \tag{6}$$

The optical conductivity (σ_{op}) was determined using the relation [23]:

$$\sigma_{op} = \frac{\alpha n c}{4\pi} \tag{7}$$

where c is the velocity of light.

3. Results and discussion

The RBS experimental and simulated plot for sample Ts333, pH1.5 (NB) is given in Fig. 1. The peaks for Sn, Cu and S at 2199 keV, 1974 keV, and 1562 keV, respectively, are energies as seen by the detector after the backscattering from the target atoms in the film. The marked edges for Sn, Cu and S in the plot represent the backscattering from the surface of the film. The steps in the plot represent the elements in the substrates. The peak in the plot for O in the substrate represents the non-Rutherford Backscattering of He ions at 2.5 MeV. The elemental composition (at %) and the thickness of the film (10^{15} at/cm^2) was obtained by simulating the experimental plot with SIMNRA computer program [18]. A depth scale of 10^{15} atoms/cm^2 is the characteristics of RBS analysis, which is the total number of atoms visible to the incident beam. If the sample density is known, this parameter can be converted to the actual thickness of films in nm. Since the film density could not be calculated accurately, therefore, thicknesses of the deposited films are given RBS characteristic depth scale. The elemental composition and thicknesses of thin Cu_2SnS_3 deposited films are summarised in Table 1.

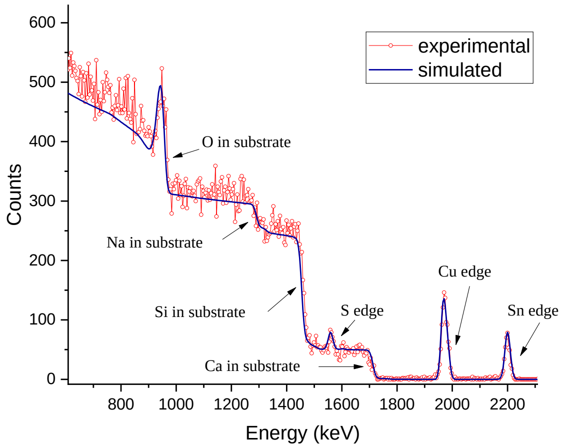

Fig. 1. A plot of RBS experimental and simulated for sample T_s=333,pH=1.5.

The RBS results indicated that the samples are mostly Cu- rich, and S- poor and the elemental concentrations of Cu, Sn, and S do not match the stoichiometric ratio of Cu_2SnS_3. Therefore, we expect the presence of a Cu_2SnS_3 phase along with the secondary phases like Cu_2S or SnS in the film. However, the concentrations in the deposited film, Cu_2SnS_3 (real phase) was improved when substrate temperature during the deposition was increased. The increased temperature increased the surface diffusion of elements, which assisted in minimizing their energy to form a Cu_2SnS_3 phase in film. The best samples were obtained for films deposited at 343K with pH values of 1.5 and 2. These films produced a Cu_2SnS_3 phase of 72% and 60% for films T_s=343, pH=1.5 and T_s=343,pH=2.0, respectively. These results are consistent with previous results reported for Cu_2SnS_3 thin films by Zhao et.al [1]. Thicknesses of deposited films oscillate with the pH values, moreover no clear trend in thicknesses is observed with the change in substrate temperature as well, as shown in Table 1.

Table 1. Elemental composition, film thicknesses and percentage of stoichiometric Cu_2SnS_3 in deposited films at different substrate temperatures and pH.

Sample Symbol	Sample	Layer Thickness (10^{15}at/cm^2)	Fabrication Ratio %			Formula standard of moles	Real Ratio of Cu_2SnS_3 %			Formed Film %	Secondary Phases %
			Cu	Sn	S		Cu	Sn	S		
LA	Ts313,pH1.0	24	57	10	33	$Cu_{3.42}Sn_{0.6}S_{1.98}$	19.9	9.99	30	60	40
LB	Ts313,pH1.5	3.0	80	15	5	$Cu_{4.8}Sn_{0.9}S_{0.3}$	3.33	1.66	5	10	90
LC	Ts313,pH2.0	22	55	10	35	$Cu_{3.3}Sn_{0.6}S_{2.1}$	19.9	9.99	30	60	40
MA	Ts323,pH1.0	15	50	28	22	$Cu_3Sn_{1.68}S_{1.32}$	14.65	7.33	22	44	56
MB	Ts323,pH1.5	9.0	88	4	8	$Cu_{5.28}Sn_{0.24}S_{0.48}$	5.32	2.66	8	16	84
MC	Ts323,pH2.0	38	57	15	28	$Cu_{3.42}Sn_{0.9}S_{1.68}$	18.64	9.33	28	56	44
NA	Ts333,pH1.0	36	57	15	28	$Cu_{3.42}Sn_{0.9}S_{1.68}$	18.64	9.33	28	56	44
NB	Ts333,pH1.5	30	57	7	36	$Cu_{3.42}Sn_{0.42}S_{2.16}$	13.99	6.99	21	42	58
NC	Ts323,pH2.0	30	57	10	33	$Cu_{3.42}Sn_{0.6}S_{1.98}$	19.9	9.99	30	60	40
RA	Ts343,pH1.0	35	52	20	28	$Cu_{3.12}Sn_{1.2}S_{1.68}$	18.64	9.33	28	56	44
RB	Ts343,pH1.5	35	50	14	36	$Cu_3Sn_{0.84}S_{2.16}$	23.98	11.99	36	72	28
RC	Ts343,pH2.0	27	57	10	33	$Cu_{3.42}Sn_{0.6}S_{1.98}$	19.9	9.99	30	60	40

Since the deposited thin film is composed of the different phases, the optical properties will depend on the percentage of real and secondary phases. The parameters that could affect the formation of a multiphase film are the ion interactions within the solution, light, humidity, substrate temperature, pH, deposition time, and concentration of the complex agent that affects reaction speed, which can aid in the formation of secondary phases. During the deposition process, the ratio of copper was high in all experimental procedures due to the strong interaction between copper and the complex agent and the slow operation of released ions. Accordingly, some of the copper is not formed in the main films, whereas sulfur was bounded in the solution, resulting in the formation of stable cation-complexes, such as CuS. Therefore, the effect of deposition parameters plays an important role in how the single phase of the deposited film will form. These results agreed with that observed by other researchers [8]. The deviation from the stoichiometric results may be attributed to the diffusion of Sn atoms on the surface of the Cu_2SnS_3 films, which were due to the high temperature and the reaction of Sn atoms with hydrogen sulphide, where the medium of solution is acidic [5].

The optical properties of the fabricated thin Cu_2SnS_3 films, in terms of absorbance, direct energy gap, absorption coefficient, refractive index, extinction coefficient, real and imaginary dielectric constants and optical conductivity, were calculated using equations 1to7. Figure 2 represents the absorbance spectrum of the fabricated films as a function of substrate temperature and pH value. The trend of the absorbance gradually decreased with the increase of the wavelength from 350 to 750 nm in all prepared samples. The absorbance increased when substrate temperature and pH value increased, which can be attributed to the increase in thickness and the percentage of stoichiometric Cu_2SnS_3 (real phase) of the deposited film. As the pH value in the chemical solution is reduced when temperature of solution increases, the increase in the substrate temperature must be followed by an increase in the pH value. Therefore, samples with high absorbance were prepared at high substrate temperatures and high pH values. Sample T_s343, pH2.0, for example, had the highest value of absorbance, which decreased sevenfold as the wavelength increased from 350 to 750 nm. Whereas samples with lower substrate temperatures and solution pH values exhibited lower absorbance at short wavelengths and decreased four – six fold at longer wavelengths.

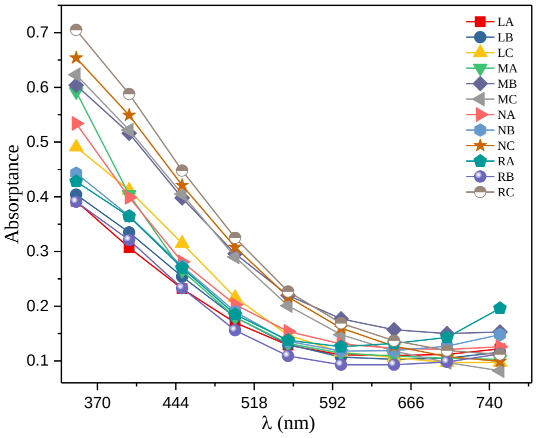

Fig. 2. The absorbance vs wavelength for nano thin Cu_2SnS_3 films at different T_s and pH.

Fig. 3 shows the absorption coefficient as a function of photon energy. The absorption coefficient values for all prepared films are >10^4 cm^{-1} which corresponds to the transition between an extended state in both valence and conduction bands, where absorption coefficient measures the intensity loss of the incident wave. It is also clear from Fig. 3 that the absorption coefficient increases when the photon energy and substrate temperature increased for films prepared at pH equal to 2. These results indicate that high values of absorption coefficient can be achieved when films are fabricated at high temperatures and high pH values. Another noteworthy observation is the eightfold increase of absorption coefficient value for samples fabricated at high pH values (for example T_s343, pH2.0, T_s333,pH2.0, and T_s323,pH2.0) with increasing photon energy. On the other hand, samples fabricated at lower pH values exhibited small changes of absorption coefficient values as a function of photon energy. According to the absorption and structural results, Sample T_s343, pH2.0 presented the optimum fabrication parameters.

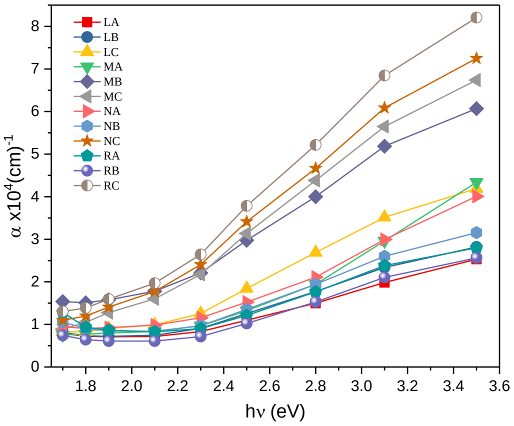

Fig. 3. The absorption coefficient vs hυ for nano thin Cu_2SnS_3 films at different T_s and pH.

Fig. 4 shows the plots of $(\alpha h\upsilon)^2$ versus hυ for sake of deducing the direct energy gap of the nano thin Cu2SnS$_3$ films. The direct band gap (E_g) values were found to vary between 2.48 to 2.58 eV depending on the deposition parameters. A summary of the direct band gap for the fabricated films is shown in Table 2. Sample T_s=343, pH=2.0 displayed the direct band gap of about 2.48 eV. It is clear from Table 2 that the energy band gap is pH dependant, as the E_g decreased with increasing the pH value for all fabricated samples, observed from the shift of $(\alpha h\upsilon)^2$ towards shorter wavelengths when the pH value was increased. The substrate temperature did not show a clear effect on E_g. The high values of the direct energy gap in all prepared samples is due to electron confinement, which is represented in the nano-scale systems [14], or differences in stoichiometric and phase, rather than the quantum size effect [24]. The E_g values that were found for the nano thin Cu_2SnS_3 films in this work are slightly greater than that found by Becerra et al (E_g= 2.15) [25] and Zhao and Cheng (E_g = 2.19) [1].

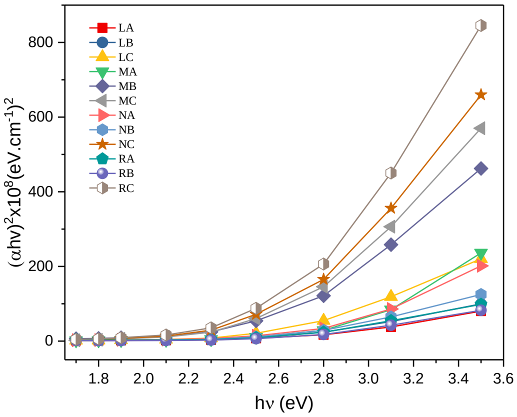

Fig. 4. $(\alpha h\upsilon)^2$ vs hυ for nano thin Cu_2SnS_3 films at different T_s and pH.

Figs. 5 and 6 showed refractive index and extinction coefficient for nano thin Cu_2SnS_3 films as a function of wavelength. Both parameters showed a clear decrease in value when increasing the wavelength up to about 600 nm, where n and κ reached almost constant values. In general, the refractive index and extinction coefficient increased when the pH value and substrate temperature were increased. Sample T_s343, pH2.0 exhibited higher values of n and κ at low wavelengths, representing energy absorption at high photon energy in the visible region. This is another indication of well-deposited film with high energy absorption suitable for optoelectronic application devices, such as solar cells. The low values of κ for all fabricated samples reflect high penetration depth of incident electromagnetic waves, while high values of *n* indicate low reflectance.

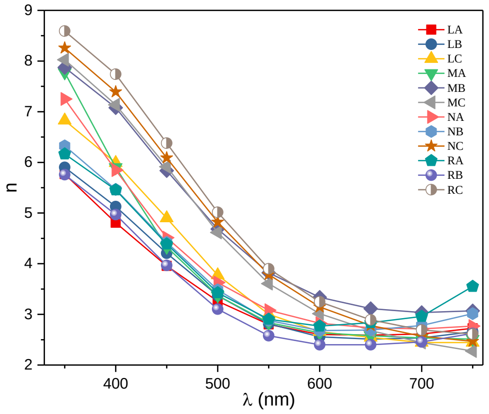

Fig. 5. Refractive index vs wavelength for nano thin Cu_2SnS_3 films at different T_s and pH.

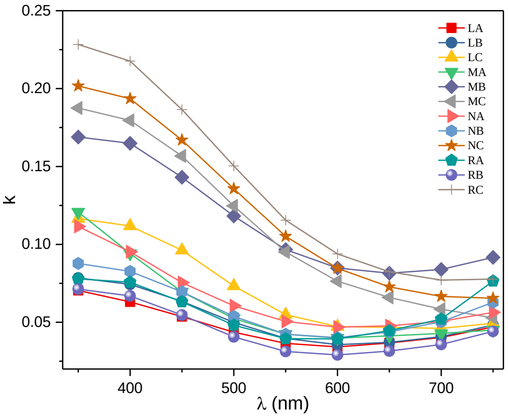

Fig. 6. Extinction coefficient vs wavelength for nano thin Cu_2SnS_3 films at different substrate temperature, T_s, and pH.

The complex dielectric constant is a fundamental property of materials. The real part is associated with controlling the velocity of light within the material, and the imaginary part gives an indication of the dielectric properties in the material resulting from the electric field produced from the polarization process. Fig. 7 illustrates the variation of real and imaginary dielectric constants for thin Cu_2SnS_3 films. The dielectric grows gradually with increasing photon energy for *hv* higher than 2 eV. The highest real and imaginary dielectric constants were observed with samples fabricated with pH solution of 2, with less dependence on substrate temperature, as shown by samples T_s323, pH2.0, T_s333, pH2.0 and T_s343, pH2.0 in Fig. 7. In addition, the value of the real part is greater than of the imaginary part. This behaviour leads to an increase of extinctions and electronic transfers through the material from valence to conduction band. Remarkably, all fabricated samples had high values of dielectric constant; this indicates that the high electronic polarization was obtained due to the interaction between incident photons and electrons at high frequencies in the visible region. Therefore, a random electronic transfer that makes electronic collisions were minimised and electronic transition was expected to be directly between valence to conduction bands.

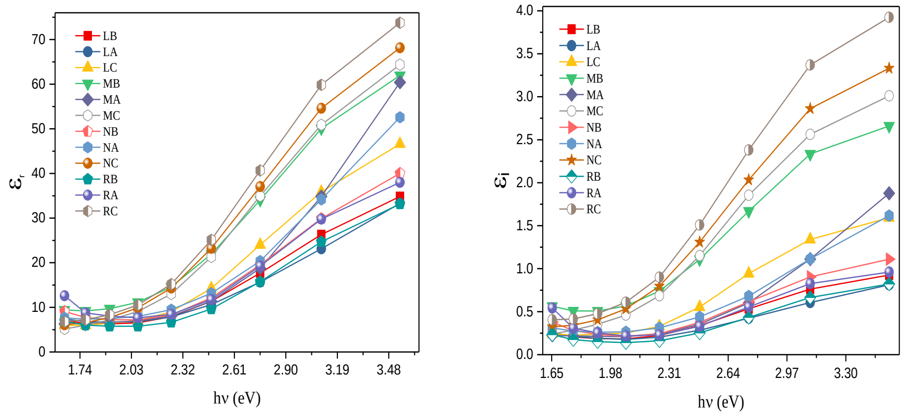

(a) *(b)*

Fig. 7. ***(****a) Real and (b) imaginary dielectric constants vs hυ for thin Cu_2SnS_3 films at different T_s and pH.*

From the calculated values of α and *n*, and reference to Eq. 7, the optical conductivity was calculated as a function of photon energy, as shown in Fig. 8. The behaviour of the optical conductivity showed a similar trend as the dielectric constant's behaviour. A clear increase at high values of pH and substrate temperatures were observed in samples T_s323, pH2.0, T_s333, pH2.0 and T_s343, pH2.0. This high value of optical conductivity is an indication of a high optical response at high frequencies of the visible region, leading to high electronic polarization due to bonded charges or ions. The electronic polarisation in such material is expected to produce dipole momentums that will create an alternating electric field. Such electric fields produce oscillating conduction of electrons around their equilibrium positions without net transnational motion. These electrons are considered a part of the dielectric medium.

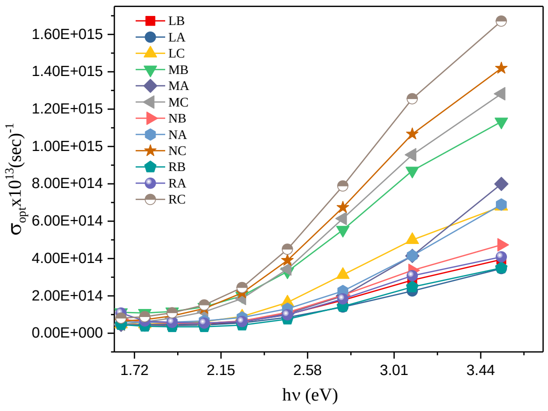

Fig. 8. Optical conductivity vs hυ for thin Cu_2SnS_3 films at different T_s and pH.

Table 2. Optical parameters (E_g, $\lambda_{cuttoff}$, n, κ, α, ε_i, ε_r, and σ_{op}) for nano thin Cu_2SnS_3 films at different T_s and pH values with 80 min. deposition time.

Sample Symbol	Sample	E_g (eV)	$\lambda_{cuttoff}$ (nm)	values at λ = 550 nm					
				n	κ	α (cm^{-1})	ε_r	ε_i	σ_{op}(sec^{-1})
LA	Ts313,pH1.0	2.58	480	2.80	0.0364	$8.33x10^3$	7.84	0.204	$5.53\ x10^{13}$
LB	Ts313,pH1.5	2.54	488	2.81	0.186	$4.26\ x10^4$	7.86	1.05	$2.84\ x10^{14}$
LC	Ts313,pH2.0	2.50	496	3.00	0.0550	$1.25\ x10^4$	9.00	0.329	$8.89\ x10^{13}$
MA	Ts323,pH1.0	2.58	480	2.83	0.0423	$9.68\ x10^3$	8.01	0.239	$6.49\ x10^{13}$
MB	Ts323,pH1.5	2.50	496	3.82	0.0967	$2.21\ x10^4$	14.5	0.739	$2.00\ x10^{14}$
MC	Ts323,pH2.0	2.48	500	3.60	0.0951	$2.17\ x10^4$	12.9	0.685	$1.85\ x10^{14}$
NA	Ts333,pH1.0	2.58	480	3.08	0.0505	$1.16\ x10^4$	9.48	0.311	$8.47\ x10^{13}$
NB	Ts333,pH1.5	2.55	486	2.88	0.0423	$9.68\ x10^3$	8.29	0.244	$6.61\ x10^{13}$
NC	Ts323,pH2.0	2.50	496	3.78	0.105	$2.41\ x10^4$	14.28	0.794	$2.16\ x10^{14}$
RA	Ts343,pH1.0	2.55	486	2.90	0.0395	$9.02\ x10^3$	8.41	0.229	$6.20\ x10^{13}$
RB	Ts343,pH1.5	2.53	490	2.58	0.0312	$7.14\ x10^4$	6.66	0.161	$4.37\ x10^{14}$
RC	Ts343,pH2.0	2.48	500	3.90	0.116	$4.26\ x10^4$	15.2	0.905	$3.94\ x10^{14}$

4. Conclusion

Thin Cu_2SnS_3 films with different substrate temperatures and pH values have been deposited on a glass substrate using a chemical bath deposition technique at the constant deposition time of 80 minute. Compositions of real and secondary phases of Cu_2SnS_3 for all fabricated samples have shown similar concentrations as those in the fabrication conditions. In particular, films fabricated with the substrate temperature of 343 K and solution pH of 2 and 1.5 exhibited real phase of 60% and 72%, respectively. These results were also confirmed from the optical properties; optical energy gap = 2.48 eV with optical constants n = 3.9, κ = 0.116, ε_r = 15.20, ε_i = 0.9 and σ_{op}> 10^{14} at wavelength 550 nm. These are promising results for the development of next generation optoelectronic devices, such as solar cells.

References

[1] P. Zhao, S. Cheng, Advances in Materials Science and Engineering **2013**, (2013).

[2] J. Han, Y. Zhou, Y. Tian, Z. Huang, X. Wang, J. Zhong, Z. Xia, B. Yang, H. Song, J. Tang, Frontiers of Optoelectronics **7**(1), 37 (2014).

[3] M. H. Sayed, E. V. C. Robert, P. J. Dale, L. Gütay, Thin Solid Films **669**, 436 (2019).

[4] X. Chen, X. Wang, C. An, J. Liu, Y. Qian, Journal of Crystal Growth **256**(3–4), 368 (2003).

[5] M. A. S. M. Yunos, Z. A. Talib, W. M. M. Yunus, Journal of Chemical Engineering and Materials Science **2**(7), 103 (2013).

[6] P. A. Fernandes, P. M. P. Salomé, A. F. Da Cunha, Journal of Physics D: Applied Physics **43**(21), 215403 (2010).

[7] Q. Chen, D. Ma, International Journal of Photoenergy **2013**, (2013).

[8] M. Adelifard, M. M. B. Mohagheghi, H. Eshghi, Physica Scripta **85**(3), 35603 (2012).

[9] V. P. G. Vani, R. W. Miles, K. T. R. Reddy, Journal of Optoelectronic Engineering **3**, 1 (2013).

[10] B.Y.taher,M.F.A.Alias,I.S.naji,A.A.Alnajjar, Chalcogenide Letters **16**(7),351 (2019).

[11] S. N. A. Kassim, H. S. Mind, T. W. Tee, A. Sharif, Z. Y. Kuang , M. J. Haron, Cmu. J. Nat. Sci. **7**, 317 (2008).

[12] K. Anuar, W. Tan, M. Atan, The Pacific Journal **8**, 252 (2007).

[13] S. N. A. Kassim, Z. Kuang, A. Sharif, T. W. Tee, H. Min, Indian Journal of Eng. and Mat. Sc **17**, 295 (2010).

[14] M. F. A. Alias, I. S. Naji, B. Y. Taher, A. A. J. Al-Douri, Journal of Non-Oxide Glasses

8(4), 93 (2016).
[15] I. S. Naji, M. F. A. Alias, B. Y. Taher, A. A. J. Al-Douri, Chalcogenide Letters **15**(2),83 (2018).
[16] N. Ghobadi, International Nano Letters **3**(1), 2 (2013).
[17] A. A. J. Al-Douri, B. Y. Taher, M. F. A. Alias, I. S. Naji, H. Alawadhi, Australian Journal of Basic and Applied Sciences **9**, 406 (2015).
[18] J. F. Ziegler, M. D. Ziegler, J. P. Biersack, Nuclear Instruments and Methods in Physics Research, Section B: Beam Interactions with Materials and Atoms **268**(11–12), 1818 (2010).
[19] A. Goswami, Thin film fundementals, New Age international Pvt.Ltd, New Delhi, 442 (1996).
[20] R. M. Mane, R. R. Kharade, N. S. Patil, P. N. Bhosale, Archives of Applied Science Research **2**(2), 275 (2010).
[21] M. N. M. Alias, Iraqi Journal of Physics **7 (9)**, 67 (2009).
[22] M. N. M. Alias, M. F. A., H. Kh. Alamy, Renewable energy **24**, 341 (2001).
[23] E. Márquez, A. M. Bernal-Oliva, J. M. González-Leal, R. Prieto-Alcón, A. Ledesma, R. Jiménez-Garay, I. Mártil, Materials Chemistry and Physics **60**(3), 231 (1999).
[24] G. Hodes, Chemical Solution Deposition of Semiconductor Films, Marcel Dekker Inc., Basel, New Yourk, 376 (2003).
[25] R. A. Becerra, J. M. Correa, H. Suarez, G. Gordillo, Journal of Physics: Conference Series, **480**(1), 12008 (2014).